EFFECT OF METAL OXIDE NANOPARTICLE ON CURING KINETIC OF BIORESIN

WAN NURUL NAJIHAH BINTI WAN GHAFAR

BACHELOR OF CHEMICAL ENGINEERING
UNIVERSITI MALAYSIA PAHANG

Thesis Access Form

No_____________________________Location________________________________

Author : ………………………………

Title : ………………………………

Status of access OPEN / RESTRICTED / CONFIDENTIAL

Moratorium period:______________ years, ending___________/_______200____

Conditions of access proved by (CAPITALS): PM DR MD MAKSUDUR RAHMAN KHAN

Supervisor (Signature)………………………………………………

Faculty: ………………………………

Author's Declaration: *I agree the following conditions:*

OPEN access work shall be made available (in the University and externally) and reproduced as necessary at the discretion of the University Librarian or Head of Department. It may also be copied by the British Library in microfilm or other form for supply to requesting libraries or individuals, subject to an indication of intended use for non-publishing purposes in the following form, placed on the copy and on any covering document or label.

*The statement itself shall apply to **ALL** copies:*

This copy has been supplied on the understanding that it is copyright material and that no quotation from the thesis may be published without proper acknowledgement.

Restricted/confidential work: All access and any photocopying shall be strictly subject to written permission from the University Head of Department and any external sponsor, if any.

Author's signature……………………………………….Date: ………………………………

users declaration: for signature during any Moratorium period (Not Open work):
I undertake to uphold the above conditions:

Date	Name (CAPITALS)	Signature	Address

EFFECT OF METAL OXIDE NANOPARTICLE ON CURING KINETIC OF BIORESIN

WAN NURUL NAJIHAH BINTI WAN GHAFAR

Thesis submitted in partial fulfilment of the requirements
for the award of the degree of
Bachelor of Chemical Engineering

Faculty of Chemical & Natural Resources Engineering
UNIVERSITI MALAYSIA PAHANG

JUN 2015

SUPERVISOR’S DECLARATION

We hereby declare that we have checked this thesis and in our opinion, this thesis is adequate in terms of scope and quality for the award of the degree of Bachelor of Chemical Engineering.

Signature :
Name of main supervisor : MD MAKSUDUR RAHMAN KHAN
Position : ASSOCIATE PROFESSOR
Date :

STUDENT'S DECLARATION

I hereby declare that the work in this thesis is my own except for quotations and summaries which have been duly acknowledged. The thesis has not been accepted for any degree and is not concurrently submitted for award of other degree.

Signature :
Name : WAN NURUL NAJIHAH BINTI WAN GHAFAR
ID Number : KA11127
Date :

Dedication

To my family, thank you for your endless support.

ACKNOWLEDGEMENT

I would like to thanks the following people and organisations;

- My family for supporting me to finish up my research.
- My supervisors PM Dr Maksudur Rahman Khan for his guidance through the semester.
- Mr Ong Huei Ruey, postgrad students who always help and guide me to finish up the work.
- My friends for giving so much help and guidance when I need it.

ABSTRACT

Development of polymers from renewable resources have received great scientific attention. Amongst different renewable resources, plant oils have attracted much attention as raw materials for chemical industry. Vegetable oils have been utilized in the synthesis of various polymeric resin such as alkyd resins and polyester. Alkyd resins find an extensive applications in surface-coating, adhesive and composite materials. Alkyd resins were blended with other suitable resins to overcome problems such as low mechanical strength, low hardness, low thermal stability, and long curing time. Polymer nanocomposite based on nanoparticles such as metal oxide are being developed. Nanoparticles are reported to have strong impact on thermal, mechanical, electrical barrier, and flame retardant properties on nanocomposite. In the present study, alkyd resin was prepared from the vegetable oil (ratio of Palm oil to Jatropha oil at 1:1) via two stage method (alcoholysis-polyesterification). The alkyd resin was mixed with commercial epoxy resin to form a blend mixture. Apart from that, zinc oxide (ZnO) nanoparticle was mechanically mixed with the blend to form alkyd-epoxy-ZnO. Prior to that, ZnO was synthesized using a simple precipitation method. The as-prepared ZnO was characterized by X-ray diffraction (XRD) and the crystallite size was calculated by using Debye-Scherrer's equation. Scanning electron microscopy (SEM) was used to characterize the morphologies of the sample. The curing kinetic of alkyd-epoxy-ZnO blend was investigated by using non-isothermal differential scanning calorimetry (DSC) method. The effect of alkyd/epoxy ratio and ZnO nanoparticle loading on curing enthalpy was investigated. From DSC results, the peak temperature, T_p is used to calculate the activation energy, E_a by using Kissinger and Ozawa method. In addition, thermogravimetric analysis (TGA) was carried out to study the thermal degradation of the nanocomposites. The interaction between ZnO nanoparticles and the alkyd/epoxy blend were recorded by Fourier-transform infrared (FTIR). All the results from the analysis deduce a conclusion that the ZnO nanoparticles have significant effects on the performance characteristics of alkyd/epoxy blends.

ABSTRAK

Pembangunan polimer daripada sumber yang boleh diperbaharui telah mendapat perhatian saintifik yang besar. Di antara sumber yang boleh diperbaharui, minyak tumbuhan telah menarik perhatian sebagai bahan mentah untuk industri kimia. Minyak sayuran telah digunakan dalam sintesis pelbagai resin polimer seperti resin alkyd dan poliester. Resin alkyd mempunyai aplikasi yang luas dalam permukaan salutan, pelekat dan bahan komposit. Resin alkyd telah dicampur dengan resin lain yang sesuai untuk mengatasi masalah seperti kekuatan mekanikal rendah, kekerasan rendah, kestabilan haba yang rendah, dan masa pengawetan panjang. Polimer nanokomposit berdasarkan nanopartikel seperti oksida logam sedang dibangunkan. Nanopartikel dilaporkan mempunyai kesan yang kuat terhadap haba, mekanikal, elektrik halangan, dan sifat-sifat kalis api pada nanokomposit. Dalam kajian ini, resin alkyd telah disediakan daripada minyak sayuran (nisbah minyak sawit kepada minyak Jatropha; 1: 1) melalui dua kaedah peringkat (alkoholisis-polyesterification). Resin alkyd dicampur-campur dengan resin epoksi komersil untuk membentuk campuran gabungan. Selain itu, zink oksida (ZnO) nanopartikel dicampur dengan campuran untuk membentuk alkyd-epoxy-ZnO. Sebelum itu, ZnO telah disintesis dengan menggunakan kaedah pemendakan mudah. ZnO yang disediakan telah dicirikan oleh pembelauan sinar-X (XRD) dan saiz kristalnya dikira dengan menggunakan persamaan Debye-Scherrer. Mikroskop imbasan elektron (SEM) telah digunakan untuk ciri-ciri morfologi sampel. Kinetik menyembuhkan campuran alkyd-epoxy-ZnO disiasat dengan menggunakan kaedah bukan sesuhu kalorimeter pengimbasan perbezaan (DSC). Kesan nisbah alkyd / epoksi dan ZnO nanopartikel pada menyembuhkan entalpi dikaji. Dari keputusan DSC, suhu puncak, Tp digunakan untuk mengira tenaga pengaktifan, Ea dengan menggunakan kaedah Kissinger dan Ozawa. Di samping itu, analisis Termogravimetri (TGA) telah dijalankan untuk mengkaji degradasi terma nanokomposit. Interaksi antara partikel nano ZnO dan gabungan alkyd / epoksi telah direkodkan oleh Fourier-mengubah inframerah (FTIR). Semua keputusan daripada analisis disimpulkan bahawa nanopartikel ZnO mempunyai kesan yang besar ke atas ciri-ciri prestasi campuran alkyd / epoksi.

TABLE OF CONTENTS

LIST OF FIGURES

LIST OF TABLES

LIST OF ABBREVIATIONS

DSC	Differential scanning calorimetry
EDS	Energy dispersive spectra
EJO	Epoxidised jatropha oil
FTIR	Fourier-transform infrared
MEKP	Methyl ethyl ketone peroxide
SEM	Scanning electron microscopy
TGA	Thermogravimetric analysis
XRD	X-ray diffractometer

1 INTRODUCTION

1.1 Background, motivation and statement of problem

Sustainable economic growth needs guaranteed sources of raw materials for the industrial production. Nowadays, petroleum, a non-renewable resource is the most important source of industrial chemicals. As petroleum sources are been exhausted and causes environmental pollutions, there is a growing effort to make biomass as an alternative source of raw materials for sustainable growth. Polymers are an important class of industrial product and are mainly been synthesized from petroleum based raw materials which need to be replaced by the bio-based raw materials to make it sustainable. One of the industrial polymers is alkyd resin which is also known as bioresin. Bioresin is a polyester comprising of one or more reacted di-acid monomer units and one or more reacted diol monomer units where at least one of the reacted di-acid monomer units or at least one of the reacted diol monomer units is a bio-monomer obtained from a plant or an animal source (Urban & Owada, 2012). Alkyd resins are formed from the polymeric condensation of polyhydric alcohols, polybasic acids and monobasic fatty acids. Alkyds are used in the formulation of paints, varnishes, lacquers and other finishes, which make alkyd resins as a necessary raw material (Odetoye T. O., 2012). Alkyd resins are used in surface coating and composite formation due to their good characteristic such as strength, flexibility, gloss retention, good thermal stability and low price (Ling, 2014).

Oil is one of the important raw materials used in the production of oil modified alkyd resins. Vegetables oils are commonly and widely used in the manufacture of oil modified alkyd resins. Alkyd resin can be synthesized from both edible and non-edible vegetable oil sources. Non-edible oil is preferred to be used as an alternative source to synthesis alkyd resin due to its lack of food value. Among non-edible oils, jatropha (Kumar, Yaakob, Maimunah, Siddaramaiah, & Abdullah, 2010), nahar (Dutta, 2004), yellow oleander (Deka. D.C., 2011) and karanja (*Milllettia pinnata*) (Bora, Deka, Ahmed, & Kakati, 2014) oil are been investigated as potential source for the preparation of oil modified alkyd resin. Alkyd resin can significantly reduce or remove the risk associated with cross-linking agents used in other resin systems, such as sulphur in furan based resins. By using plant oils, it can creates polymers with a greater intra-chain length compared to the traditional resins. On curing, this property produces a structure that can be less brittle (providing flexibility before mechanical failure) allowing for improved impact resistance in structural applications.

Malaysia is rich in palm oil production, which known as non-drying oil due to the presence of low degree of unsaturation. Unsaturated oils are been preferred to produce bioresin due to the higher degree of cross-linking through the double bonds. Jatropha oil is one of the promising raw materials for bioresin synthesis, as it contains a high percentage of monounsaturated oleic (44.7%) and polyunsaturated linoleic acids (32.8%) (E., Z., S.K., M., & J., 2009) indicating a semi-drying property (Odetoye T. O., 2012). To the authors knowledge, there is no study reported the blending of palm oil with jatropha oil to produce bioresin. However, the blending of non-drying oil with semi-drying oil might increase the curing rate of the non-drying oil.

Furthermore, in recent years, metal nanoparticles are extensively studied to enhance the properties of the nanocomposites made from the bioresin. Pronob et al. reported the use of NiO nanoparticle on the properties of Jatropha oil based alkyd resin and epoxy blend, where the incorporation of the nanoparticle reduced the mobility of the polymer chain and increased the mechanical properties by many times. Zinc oxide nanoparticle, a multifunctional inorganic material, has drawn attention in recent years due to its outstanding physical and chemical properties, such as chemical stability, low dieletric constant, high luminous transmittance, high catalyst activity, effective antibacterial and bactericide, intensive ultraviolet and infrared absorption. Moreover, the incorporation of ZnO nanoparticles could improve the mechanical and optical properties of the polymer matrix (Omid, et al., 2011). However, the curing behaviour of the alkyd resin or the resin blends by incorporation of the metal oxide nanoparticles are not reported well throughout the literature. Hence in the present study attempts were made to prepare bioresin from jatropha and palm oil blend (1/1 wt % ratio) and the effect of ZnO nanoparticle on the curing behaviour of the composite have been investigated. Furthermore, bioresin/epoxy blend and its curing behaviour with and without ZnO nanoparticle have been studied.

1.2 Objectives

The following are the objective of this research:

- To study the effect of zinc oxide nanoparticle on the curing kinetic of bioresin.

1.3 Scope of this research

The following are the scope of this research:

i) To synthesized nanoparticles through sol gel method. The prepared nanoparticle was applied as catalysts during curing process.
ii) To synthesized bioresin by using two stages of alcoholysis-polyesterification method by mixing palm oil, jatropha oil, glycerol and phthalic anhydride.
iii) To prepared nanocomposite by mixing bioresin and nanoparticles via ultrasonic method. The curing kinetics of nanocomposite was investigated by using DSC method and its durability is checked by antimicrobial test.

1.4 Organisation of this thesis

The structure of the reminder of the thesis is outlined as follow:

Chapter 2 provides a description of preparation method of alkyd resin from various type of non-edible vegetable oil such as yellow oleander (*Thevetia peruviana*), karanja (*Millettia pinnata* (L.) Panigrahi) and jatropha *curcas* Linneaus. Fatty acid composition of Jatropha curcas oil seed, palm kernel oil, sunflower oil, soybean oil and palm oil was compared. Blending of oil modified alkyd resin with synthetic resin such as epoxy, acrylic and melamine was observed. The preparation and characterization of blends of alkyd resin and palm oil also been studied. Various physico-chemical properties such as density, viscosity, drying time, acid value, peroxide value and dry extract are observed. The effect of zinc oxide (ZnO) nanoparticle on the thermal degradation kinetics and mechanical properties of epoxy resin and nickel oxide (NiO) nanoparticles on the performance characteristics of the Jatropha oil based alkyd and epoxy blends have been reported. The curing behaviour of the resin was analysed by differential scanning calorimeter (DSC).

Chapter 3 gives a review on the process to study the effect of zinc oxide nanoparticles on curing kinetic of alkyd resins. The process starts from the synthesis of zinc oxide nanoparticles by using sol-gel method, synthesis of alkyd resin from vegetable oil by using two stages alcoholysis-polysterification and preparation of alkyd/epoxy blend and alkyd/epoxy/ZnO nanocomposite by mechanical blending method. The structure and morphologies of ZnO nanoparticles was characterized by x-ray diffraction (XRD) and scanning electron microscopy (SEM) while the blending alkyd and the nanocomposite was characterized by differential scanning calorimeter (DSC), fourier transform infrared (FTIR) spectra and thermogravimetric analysis (TGA).

Chapter 4 discuss on the result obtained from the analysis of x-ray diffraction (XRD), scanning electron microscopy (SEM), differential scanning calorimeter (DSC), fourier transform infrared (FTIR) spectra and thermogravimetric analysis (TGA). The effect of alkyd/epoxy ratio and ZnO nanoparticle loading on curing enthalpy was investigated. From DSC results, the peak temperature, T_p is used to calculate the activation energy, E_a by using Kissinger and Ozawa method.

Chapter 5 draws together a summary of the thesis and outlines the future work which might be derived from the model developed in this work.

2 LITERATURE REVIEW

2.1 Overview

This chapter presents the preparation method of alkyd resin from various type of non-edible vegetable oil. Fatty acid composition of jatropha curcas oil seed, palm kernel oil, sunflower oil, soybean oil and palm oil was compared. The preparation and characterization of blends of alkyd resin with synthetic resin and palm oil also been studied. Various physico-chemical properties such as density, viscosity, drying time, acid value, peroxide value and dry extract are observed. The effect of zinc oxide (ZnO) nanoparticle on the thermal degradation kinetics and mechanical properties of epoxy resin and nickel oxide (NiO) nanoparticles on the performance characteristics of the Jatropha oil based alkyd and epoxy blends was reported. The curing kinetic of the blend was studied by using DSC.

2.2 Preparation of alkyd resins from vegetable oils

Alkyd resin is a key ingredient of all surface coating products due to their good attributes such as strength, flexibility, gloss retention, good thermal stability and low price. It can be synthesized from both edible and non-edible oil vegetable oil sources. Non-edible vegetable oil is chosen as it has no competing food uses. Bora et al. reported synthesis of alkyd resins from yellow oleander (*Thevetia peruviana*). The resin possess gratifying gloss, hardness, adhesion, chemical resistance and thermal stability which make them suitable for surface coating and binder for composite. The study reveals that yellow oleander seed oil is a good source of renewable raw material having the potential to synthesize alkyd resins for the coating industry (Bora, Gogoi, Deka, & Kakati, 2014). Bora et al. also reported the synthesis of alkyd resin from karanja (*Millettia pinnata (*L.) Panigrahi) seed oil. The karanja seed oil possesses the characteristics of a non-drying oil, for which the successful application of its alkyd resins as coating materials requires its blending with epoxy resin and epoxy hardener and curing. The physical properties of the cured epoxy-blended resin conform to the required standard for suitable application as coating material. Hence, karanja seed oil, a non-edible oil, provides a renewable sources of raw materials for production of alkyd resin, for subsequent use as coating material (Bora, Deka, Ahmed, & Kakati, 2014). Odetoye et al. reported the preparation and evaluation of jatropha *curcas* Linneaus seed oil alkyd resin. The study reveals that oil extracted from the seeds of jatropha *curcas* Linneaus is a potential raw material for the coatings industry. Some properties of the alkyds compare favourably with those of the commercial standards while *Jatropha* oil alkyds exhibited outstanding colour and gloss (Odetoye, Ogunniti, & Olatunji, 2010).

Emil et al. study the characteristic and composition of jatropha curcas oil seed from Malaysia. They study the psycho-chemical properties including the fatty acids of the jatropha oil seed. Table 2-1 below shows the comparison of the fatty acid composition of Jatropha curcas oil seed, palm kernel oil, sunflower oil, soybean oil and palm oil.

Table 2-1 Fatty acid composition %

Fatty Acid	Jatropha curcas oil seed	Palm kernel oil	Sunflower oil	Soybean oil	Palm oil
Oleic 18:1	44.7	15.4	21.1	23.4	39.2
Linoleic 18:2	32.8	2.4	66.2	53.2	10.1
Palmitic 16:0	14.2	8.4	-	11.0	44.0
Stearic 18:0	7.0	2.4	4.5	4.0	4.5
Palmitoliec 16:1	0.7	-	-	-	-
Linolenic 18:3	0.2	-	-	7.8	0.4
Arachidic 20:0	0.2	0.1	0.3	-	-
Margaric 17:0	0.1	-	-	-	-
Myristic 14:0	0.1	16.3	-	0.1	1.1
Caproic 6:0	-	0.2	-	-	-
Caprylic 8:0	-	3.3	-	-	-
Lauric 12:0	-	47.8	-	-	0.2
Capric 10:0	-	3.5	-	-	-
Saturated	21.6	82.1	11.3	15.1	49.9
Monounsaturated	45.4	15.4	21.1	23.4	39.2
Polyunsaturated	33	2.4	66.2	61.0	10.5

(Edem, 2002)

Based on the comparison table of vegetable oils above, the major fatty acids in Jatropha seed oil were the oleic, linoleic, palmitic and the stearic fatty acid. Oleic acid showed the highest percentage of composition of 44.7% followed by linoleic acid with 32.8%. Thus, Jatropha seed oil can be classified as oleic–linoleic oil. Compared to others vegetable oil, Jatropha oil seed has highest oleic contain than palm oil, palm kernel, sunflower, coconut and soybean oil. This indicates the semi drying properties of Jatropha oil.

2.3 *Blending of oil modified alkyd resin with the synthetic resin*

Some major drawbacks of vegetable oil based alkyd resins such as low mechanical strength, low hardness, low thermal stability, and long curing time limits their practical application. To overcome these drawbacks, alkyd resins were blended with other suitable resins such as epoxy resin, amino resin, silicone resin and ketonic resin. Dutta et al. reported the preparation of alkyd/epoxy blends as multipurpose coatings. The alkyd/epoxy blends showed better performance in terms of drying time, hardness, flexibility, gloss, thermal stability and chemical resistance (Dutta, 2004). Wang et al. reported the development of alkyd/acrylic blends for the creation of hard coatings. However, alkyd resin and acrylic phase was found to be more compatible in alkyd/acrylic hybrid latex than the alkyd/acrylic blends (Wang, et al., 2010). Radicevic and Simendic reported the preparation of alkyd/melamine resin blends with various ratio of melamine. It was observed that the degree of curing alkyd/melamine resin blends increases with increasing the ratio of melamine in the blends (Radicevic & Simendic, 2005).

Blaise et al. reported preparation and characterization of blends of alkyd resin and palm oil by studying various physico-chemical properties. These properties are density, viscosity, drying time, acid value, peroxide value and dry extract. The results show that palm oil contributed to the increase of drying times of the blends; this development is attributed to the relative saturation of palm oil included in the blend. However, density and viscosity of the blends decreased as the palm oil content in the blend increased. Since the viscosity of the blend is lower compared to that of the pure alkyd, it is not likely to produce a hard film, but it may be suitable for paint systems which require low viscosity. Also, it was observed that the inclusion of palm oil led to increase in the dry extract which may also affect the thickness of alkyd resin. Contrary to the peroxide value which decrease, the acid value increase with increase of palm oil in the blend. The results suggest that palm oil can be used as a blending additive for coating formulations.

Table 2-2 Property of alkyd resin blended with different percentages of palm oil

Property	% of palm oil in the blend with alkyd resin					
	0	10	20	30	40	50
Density	0.957	0.943	0.942	0.938	0.934	0.929
Dry extract (%)	3	4	5	80	82	84
Viscosity (cps)	5000	5000	2928	1413	779	499
Drying time (h)	4	5	7	8	24	24
Gloss (%)	87.08	86.68	86.45	25.48	23.48	17.78

(Blaise, Ogunniyi, Ongoka, Moussounga, & Ouamba, 2012)

2.4 *Curing behaviour of the resins*

2.4.1 Curing of the blend

Edja et al. reported the synthesis, characterization, and performance characteristics of alkyd resin based on *Ricinodendron heudelotoii* oil and their blending with epoxy resins. The synthesized alkyd resins were blended with epoxy resin and methyl-ethyl ketone peroxide (MEKP) as initiator, cobalt-octoate as accelerator and poly (amido amine) as hardener. The blends were cured at room temperature and also at 50 °C. The cured resins exhibited improved performance characteristics in term of drying time at room temperature, adhesion and pencil hardness, gloss, and chemical resistance. The cured resins exhibited good tensile strength, improved elongation at break and thermally stable up to 400 °C.

Gogoi et al. reported the blends of epoxidized alkyd resins based on jatropha oil and the epoxidized oil cured with aqueous citric acid solution. To improve the performance characteristics of the resins, the resins were blended with different wt% of epoxidized jatropha oil (EJO) and aqueous citric acid solution without the addition of any other catalyst or solvent. It was observed that the properties like curing time, chemical resistance, scratch hardness, thermal stability, and tensile strength of the alkyd resins improved significantly on blending. With 50 wt% EJO content, the thermal stability and tensile strength of the blends increased. The results indicate the strong influence of the amount of EJO and citric acid on the performance of the alkyd resins.

2.4.2 Effect of nanoparticle on curing

Zabihi et al. study the curing, thermal degradation kinetics and mechanical properties of epoxy resin based on the diglycidyl ether of bisophenol A, 2,2'-Diamino-1,1'-binaphthalaene as a hardener and ZnO as a nanofiller.

Table 2-3 The result of DSC measurements of DGEBA/DABN at different level of ZnO nanoparticles at heating rate 10 K/min

Concentration of nanofiller (phr)	Tp (°C)	Tg (°C)	ΔH_{total} (J/g)	ΔH_{total} (kJ/mol)
0	109.4	74	202.83	78.53
1	105.3	84	214.64	82.34
5	102.5	93	226.34	87.07
10	107.8	88	213.73	81.87
15	115.7	79	206.56	79.59

The higher thermal and mechanical properties were obtained with a percentage of 5 phr of ZnO nanoparticles. A two-parameter (m,n) autocatalytic model (Sěsták-Berggren equation) was found to be the most adequate selected kinetic model. In addition, the predicted curves from the kinetic model fit well with dynamic DSC thermograms. The addition of ZnO nanoparticles into the epoxy matrix resulted in a significant increment in the thermal stability and activation energy of thermal degradation. The epoxy nanocomposite exhibited an increase in storage modulus and glass transition temperature compared to the neat epoxy (Omid, et al., 2011).

Pronob reported the effect of nickel oxide (NiO) nanoparticles on the performance characteristics of the Jatropha oil based alkyd and epoxy blends. The alkyd/epoxy/NiO nanocomposites showed the gradual increase in thermal stability with increasing NiO content. With 3 wt % NiO content the tensile strength of the nanocomposites indicated that the incorporation of NiO nanoparticles even in 1 wt % can greatly improves the flame retardant properties of the alkyd/epoxy/NiO nanocomposites (Pronob & Swapan, 2014).

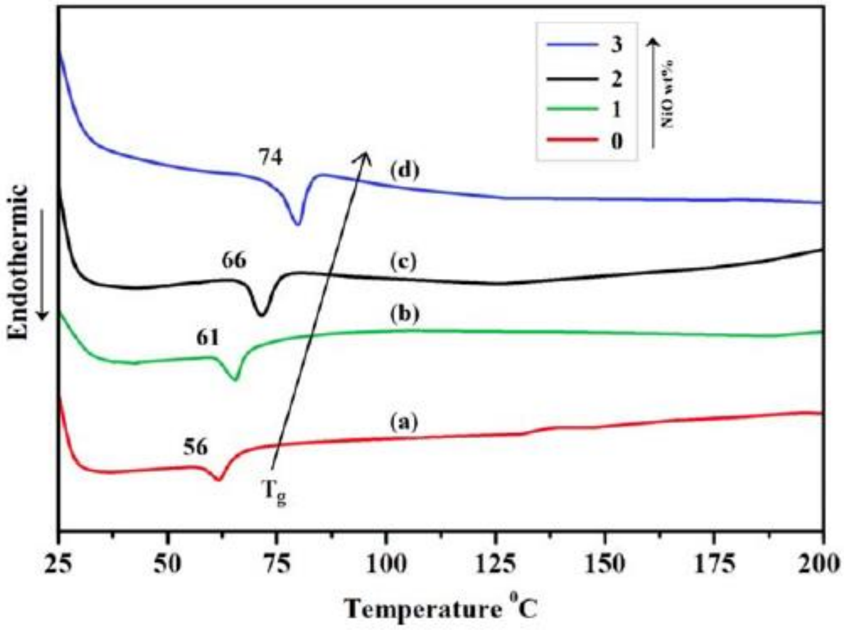

Figure 2-1 DSC traces of (a) alkyd/epoxy blend, (b) nanocomposite (1% NiO), (c) nanocomposite (2% NiO0, (d) nanocomposite (3% NiO).

Based on the results of DSC traces from DSC thermograms above, the incorporation of NiO significantly improved the glass transition temperature, Tg of the nanoparticles. The Tg increases linearly with increasing NiO content and found to be increased by 20 °C for the nanocomposite with 3% NiO when compared with the neat polymer. It can be explained by the reduced mobility of the polymer chain in the presence of NiO nanoparticles. These results clearly suggest strong interaction (dipole–dipole) between NiO nanoparticles and the polymer matrix.

Table 2-4 Mechanical properties of the nanocomposite

Entry	NiO wt %	Tensile strength (MPa)	Elastic modulus (GPa)	Elongation at break (%)	Toughness	Scratch hardness (kg)[a]
1	0	17 ± 0.42	1.26 ± 0.31	67 ± 2	825	8.3
2	1	22 ± 0.13	1.81 ± 0.43	51 ± 2	880	9.4
3	2	29 ± 0.25	1.98 ± 0.16	37 ± 2	928	>10
4	3	36 ± 0.27	2.18 ± 0.18	21 ± 2	510	>10

(Pronob & Swapan, 2014)

Mechanical properties like tensile strength, elongation at break (%), Young's modulus, and toughness of the nanocomposite films are summarized in table above. Tensile strength and elastic modulus of the nanocomposites increases linearly with increasing NiO concentration. It implies the sufficient transfer of mechanical energy from polymer matrix to the nanofiller. The mechanical energy transfer is only plausible when the nanofiller is strongly attached to the polymer matrix

2.5 Summary

This chapter propose the uses of jatropha curcas oil as the main raw material to produce alkyd resin since it has highest percentage of monounsaturated oleic acid among others which indicate a semi-drying property. Since palm oil is a non-drying oil, it has low degree of unsaturation and higher degree of cross-linking through the double bonds. The blending of non-drying oil with semi-drying oil might increase the curing rate of the non-drying oil. The use of ZnO nanoparticles as the curing agent for jatropha oil based alkyd resin as it is proven to improve the thermal and mechanical properties of the nanocomposite.

3 MATERIALS AND METHODS

3.1 Overview

In general, there are three major steps to analyse the effect of ZnO nanoparticle on alkyd resins which are synthesis of ZnO nanoparticle, synthesis of alkyd resin from vegetable oil and preparation of alkyd/epoxy/ZnO nanocomposites before it is analyse by using differential scanning calorimeter (DSC).

3.2 Materials

Phthalic anhydride, glycerol, sodium hydroxide, benzoic acid and zinc nitrate tetrahydrate of analytical grade were purchased from Sigma Aldrich and used without further purification. Jatropha oil and palm oil were obtained from local supplier.

3.3 Synthesis of Zinc Oxide (ZnO) nanoparticle

ZnO nanoparticles was prepared by using sol-gel method. 0.5 M solution of zinc nitrate and a 1.0 M alkali solution of sodium hydroxide were prepared by dissolving zinc nitrate tetrahydrate Zn(NO3)2·4H2O and NaOH, respectively, in distilled water. To prepare ZnO nanoparticles, 500 mL of the alkali solution (1.0 M NaOH) was dropped at an approximate rate of 8 mL/min into a mother solution prepared by mixing 74.50g of 0.5 M Zn(NO3)2 solution and 500.0 mL of deionized water with stirring for 12 hours. The collected product was filtered and washed several times with distilled water and dried in a vacuum oven at 100°C for several hours. The dried zinc oxide nanoparticle is then ground to fine powder using agate mortar before calcined at 300°C, 500°C, and 700°C for 2 hours in a furnace (Surabhi, Putcha, Vannka, & Gollapalli, 2013).

3.4 Synthesis of alkyd resin from the oil blend

Alkyd resin was synthesized by a two-step method from jatropha oil and palm oil (weight ratio 1:1). The first step was the alcoholysis process where monoglycerides of vegetable oil was obtained. In brief, 50g jatropha oil and 50g palm oil with 22.2g glycerol was mixed and heated to 240°C, while sodium hydroxide as catalyst (0.3 wt % with respect to oil). In the second step, the polyesterification reaction, 38.64 g of phthalic anhydride was added and the temperature was maintained at 240°C. The reaction was monitored using titration method and the reaction was stopped when the acid value dropped around 10-20 (Gogoi, Saikia, & Dolui, 2014).

Table 3-1: Composition of the ingredients to produce alkyd resins

Ingredient	Weight (g)
Jatropha oil	50
Palm oil	50
Glycerol	22.2
Sodium hydroxide (NaOH)	0.3
Phthalic anhydride	38.64

3.5 Preparation of the Alkyd/Epoxy Resin and Alkyd/Epoxy/ZnO nanocomposite

Alkyd and epoxy blends were prepared by various weight ratios of alkyd to epoxy: 0:100, 20:80, 40:60, 50:50, 60:40, 80:20 and 100:0. The alkyd/epoxy was prepared by mechanical blending. Hardener (50 wt % with respect to the epoxy resin) was added to the mixture and mechanically mixed until it is homogeneous (Gogoi, Saikia, & Dolui, 2014). The composition of the blend was presented in Table 3-2.

Table 3-2 Different ratio by mass of alkyd to epoxy resin

Resins	Alkyd (g)	Epoxy (g)	Hardener (mL)
A/E (0:100)	0	2	1
A/E (20:80)	1	4	2
A/E (40:60)	2	3	1.5
A/E (50:50)	2	2	1
A/E (60:40)	3	2	1
A/E (80:20)	8	2	1
A/E (100:0)	1	0	0

For the alkyd/epoxy/ZnO blend, similar method was adopted as above. A fixed of alkyd/epoxy (40:60) was prepared, and mixed with ZnO at different loading (0 - 8 wt %). The blend was ultrasonificated for 1.5 h to obtained homogeneous dispersion of the ZnO nanoparticles within the polymer matrix. Hardener (50 wt % with respect to the epoxy resin) was added to the mixture and mechanically mixed until it is homogeneous. The composition of the blend was presented in Table 3-3.

Table 3-3 Different wt % of ZnO nanoparticle

Sample	Epoxy (g)	Alkyd (g)	ZnO (wt%)
1	2	2	0
2	2	2	1
3	2	2	2
4	2	2	3
5	2	2	4
6	2	2	5
7	2	2	8

3.6 Characterization techniques

3.6.1 X-ray diffractometer (XRD)

The crystalline structure of ZnO nanoparticles were studied by using X-ray diffractometer (XRD) and with Cu Kα radiation ($\lambda = 0.154$ nm) at 30 kV and scanning rate of $0.005 s^{-1}$ in a 2θ range of 10°-70°.

3.6.2 Scanning electron microscopy (SEM)

The morphologies and structure of ZnO samples were taken using scanning electron microscopy (SEM).

3.6.3 Differential scanning calorimeter (DSC)

The glass transition and crystallization behaviours were investigated by differential scanning calorimeter (DSC) using TA Instruments DSC Q1000 in nitrogen atmosphere. The sample of mass between 1.7 and 2.5 mg were put into an aluminium pan and hermetically sealed. An empty pan was used as a reference. The analysis was run at a scanning speed of 10°C min^{-1} from 17 to 400°C.

3.6.4 Fourier-transform infrared (FTIR) spectra

Fourier-transform infrared (FTIR) spectra were recorded at room temperature over a frequency range of 4000-400 cm^{-1}.

3.6.5 Thermogravimetric analysis (TGA)

To study the thermal degradation of the nanocomposites, thermogravimetric analysis (TGA) was carried out in nitrogen atmosphere at a heating rate of 10°C min^{-1} in the temperature range of 25-600°C.

3.7 Kinetic analysis

Kinetic analysis of non-isothermal resin-cured system is based on the rate equation:

$$\frac{d\alpha}{dt} = \beta\frac{d\alpha}{dt} = k(T)f(\alpha)$$

where k(T) is a temperature-dependent reaction rate constant, f(α) the differential conversion function depending on the reaction mechanism, and $\beta = dT/dt$ is a constant heating rate. The rate constant, k(T) is a temperature dependant according to Arrhenius law shown in equation below:

$$k(T) = A\,exp\left(-\frac{Ea}{RT}\right)$$

Where A is the pre-exponential factor, Ea is the activation energy, and T is the absolute temperature. Non-isothermal method, a more precise measure for evaluating the curing kinetic parameters, is carried out at different heating rates. This method is very attractive because the kinetic data can be obtained in a relatively short period of time. Nevertheless, there are some complications in the mathematical analysis of the temperature integral, which are inherent to the non-isothermal approach.

The Kissinger method

Kissinger method is based on a linear relationship between the logarithms of $\beta/\mathrm{T}_\mathrm{p}^2$ and the inverse of the peak temperature of the exothermic curing reaction, through the following equation:

$$ln\left(\frac{\beta}{\mathrm{T}_\mathrm{p}^2}\right) = ln\left(\frac{Q_p AR}{E_a}\right) - \frac{E_a}{RT_p}$$

where $Q_p = -[df(\alpha)/d\alpha]_{\alpha=\alpha p}$. The activation energy (E_a) can be calculated from the slope of the linear plot of $-\ln(\beta/\mathrm{T}_\mathrm{p}^2)$ against $(1/T_p)$ (Jubsilp, Damrongsakkul, & Takeichi, 2006).

The Ozawa method

A similar method to Kissinger method is Ozawa method, which relates the logarithm of the heating rate and the inverse of the exothermic peak temperature. Therefore, the curing activation energy can be determined from the resultant slope:

$$\ln \beta = \left(\frac{AE_a}{\mathrm{R}}\right) - lnF(\alpha) - 5.331 - 1.052\left(\frac{E_a}{RT_p}\right)$$

where F(α) is a constant function (Jubsilp, Damrongsakkul, & Takeichi, 2006).

4 RESULTS AND DISCUSSIONS

4.1 *ZnO nanoparticle preparation and characterization by XRD*

ZnO nanoparticle have been prepared by method stated in the chapter above. The nanoparticle was characterized for their structure by XRD.

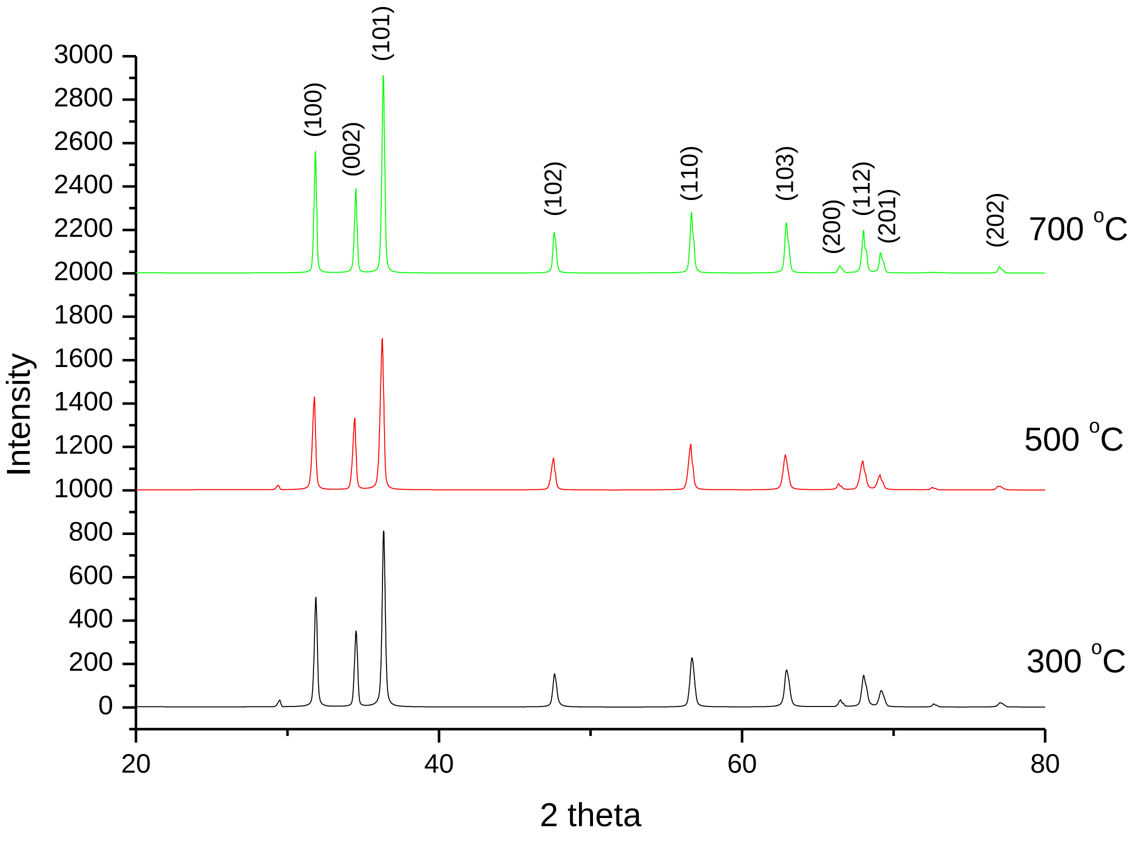

Figure 4-1 XRD patterns of ZnO calcined at different temperatures

The XRD patterns of the ZnO nanoparticle at different calcination temperature were shown in Figure 4-1. It can be seen that, there are 10 peaks (100, 002, 101, 102, 110, 103, 200, 112 201 and 202) in the XRD pattern. All peaks were well indexed to the hexagonal ZnO wurtzite structure (JCPDS no. 36-1451). Diffraction peaks corresponding to the impurity was not found in the pattern, confirming high purity of ZnO was prepared. The intensity of the peaks increases with calcination temperature was seen, indicating increased crystallinity. A definite line broadening of diffraction peaks at 300°C, 500°C and 700°C indicates that the synthesized materials are in the nanometer range. The crystallite size increases with increase in calcination temperature, similar kind trend was also obtained by (Kumar & Purushothaman, 2012) and (Ahmad, Mohammad, & Mohammad, 2012).

$$D = \frac{0.89\lambda}{\beta \cos\theta}$$

where D is the crystallite size (nm), λ is the wavelength of incident X-ray (nm), β is the full width at half maximum and θ is the diffraction angle.

Table 4-1 shows the crystallite size of the samples calculated by Debye-Scherrer's equation.

Table 4-1 Crystallite size of ZnO obtained from XRD

Calcination temperature (°C)	Crystallite size, D (nm)
300	33.99
500	41.52
700	50.69

4.2 SEM and EDS analysis

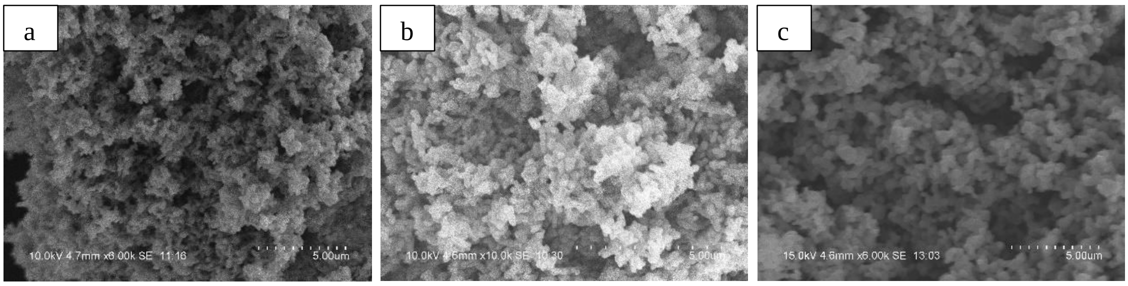

Figure 4-2 SEM images of ZnO samples calcined at three different temperatures. (a) 300 °C (b) 500 °C and (c) 700 °C

The SEM images of the prepared ZnO nanoparticles samples are shown in Figure 4-2. The morphologies of ZnO nanoparticles are changed with calcination temperature. The samples calcined at 300 °C and 500 °C are nanoflakes which are turned to particles when calcined at 700 °C. From EDX analysis (Figure 4-3), it clearly show that the sample prepared by the above route is in pure ZnO phase.

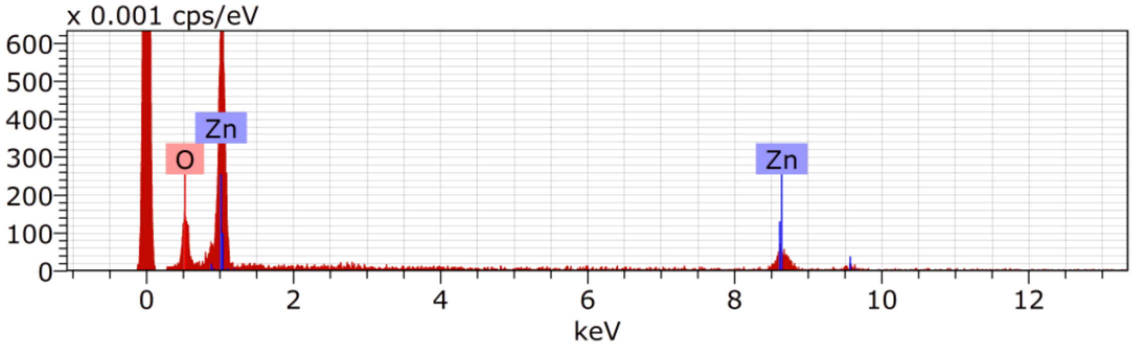

Figure 4-3 Energy dispersive spectra (EDS) of ZnO calcined at 700 °C

4.3 Preparation of alkyd resin

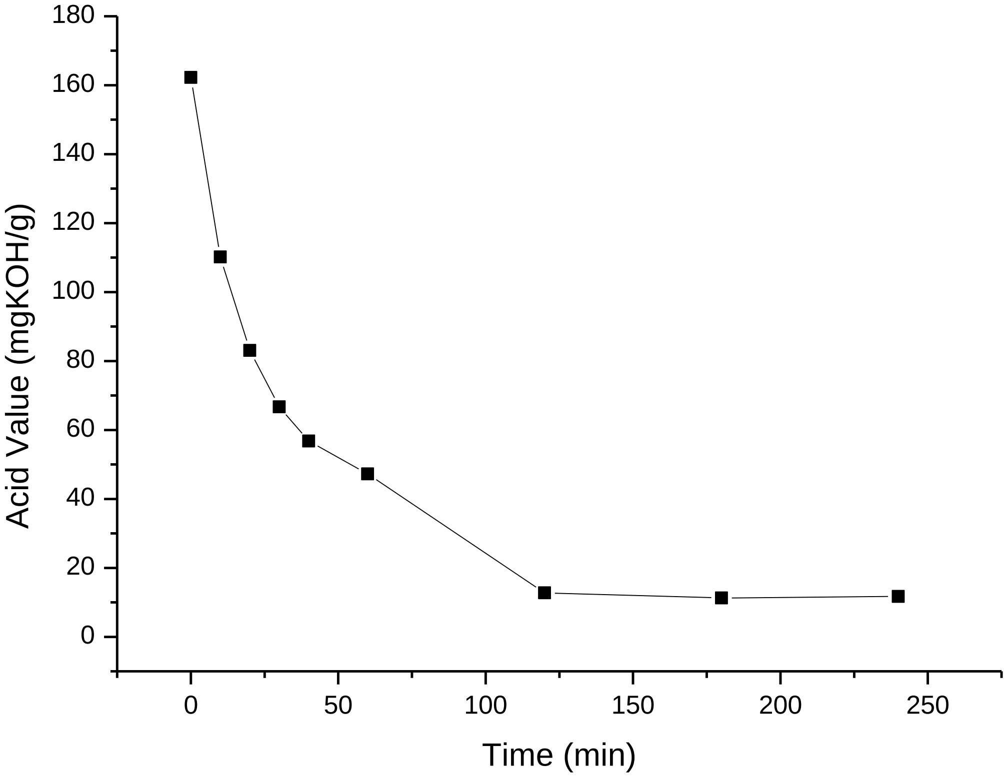

Figure 4-4 Graph of acid value for alkyd resin

The progress of reaction was monitored using titration method, where acid value (AV) was determined. The plot of AV versus reaction time was presented in Figure 4-4. It can be seen that, the decrease in acid values was more rapid during the early stages of the reaction than that during the later stages of the reaction. These changes in acid values during polyesterification reaction have been explained on the basis of different reactivity of primary and secondary hydroxyl groups of Monoglycerides (MG). Since primary hydroxyl groups react faster than secondary groups, it is believed that the rapid decrease in acid values at the early stages due to primary hydroxyl groups, while that at the later stages for secondary groups. In addition, three-dimensional network of alkyd resin is probably formed at the later stages of polyesterification due to cross-linking of alkyd chains as the viscosity of the reaction medium is increased. It is noticed that, the reaction reached equilibrium after 120 min where minimum AV was attained (~10 mgKOH/g).

4.4 Characterization of alkyd resin using DSC

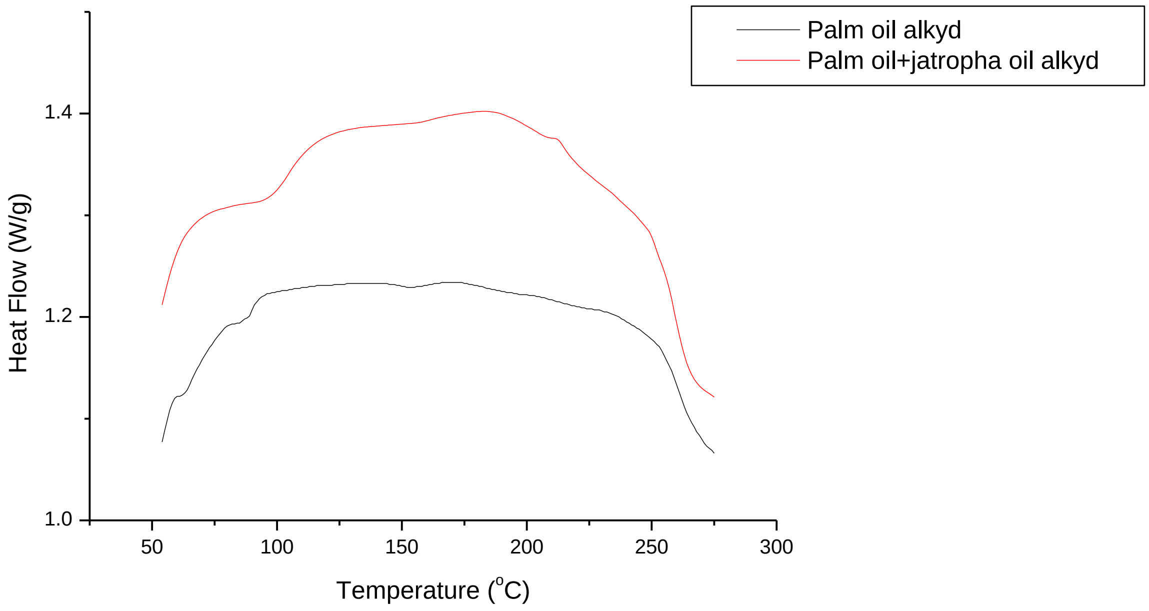

Figure 4-5 DSC thermograms of palm oil alkyd and blending of jatropha with palm oil alkyd

Figure 4-5 shows the DSC thermograms of palm oil alkyd and blending of jatropha with palm oil alkyd. The DSC curve shows that blending of jatropha oil with palm oil increase the curing curves of the resin. This proves that blending of non-drying oil (palm oil) with semi-drying oil (jatropha oil) increase the curing rate of the non-drying oil.

4.5 *FTIR spectroscopic analysis of alkyd/epoxy blend*

The FTIR transmittance spectra of epoxy neat and alkyd/epoxy blend is shown in Figure 4-6.

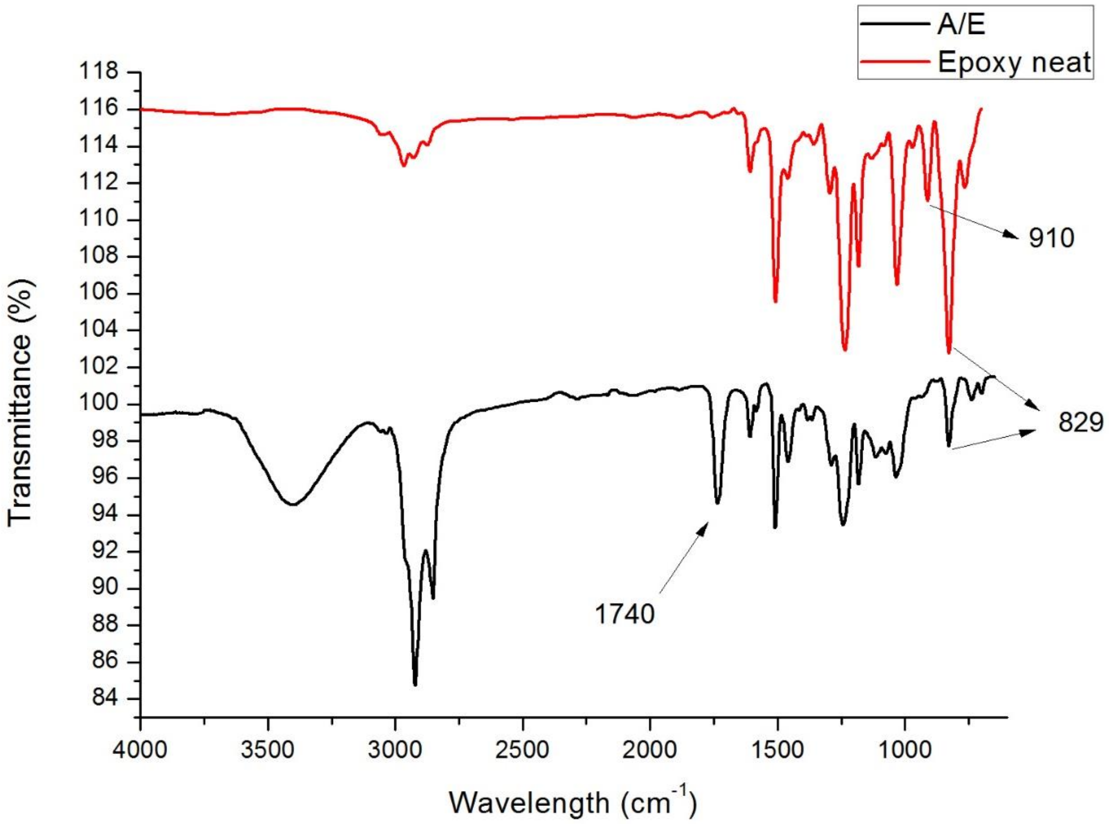

Figure 4-6 FTIR spectra of epoxy neat and alkyd/epoxy blend

The FTIR spectra were used to verify the functional group of the resin and presented in Figure 4-6. From the spectrum of epoxy, it showed a strong absorption in the region of 3030-2840 cm^{-1} due to C-H stretching. The adsorption peak at 1609 cm^{-1} and 1508 cm^{-1} were assigned to the C=C stretching of aromatic ring and C-C stretching of aromatic, respectively. The absorption peaks at 1240-1030 cm^{-1} were attributed to the C-O-C stretching of ether group. The absorption at 910 cm^{-1} and 829 cm^{-1} are attributed to stretching of C-O and C-O-C of oxirane group, respectively. The peak at 761 cm^{-1} is due to rocking of CH_2.

The FTIR spectra of alkyd/epoxy blend indicated the formation of amide bond between ester of alkyd and amine hardener, where the peak of C=O was noticed at 1740 cm^{-1}.

Apart from that, the peak intensity of C-O and C-O-C of oxirane group were reduced, especially peak at 910 cm^{-1} was diminished. This indicates the formation of network between oxirane groups with amine hardener. The peak of O-H groups became broader compared to its origin, which might be due to the formation of hydrogen bonding between hydroxyl-carbonyl.

4.6 TGA study of alkyd/epoxy blend by incorporation of ZnO

Figure 4-7 shows the TGA weight (%) loss of alkyd/epoxy blend and alkyd/epoxy ZnO nanocomposite.

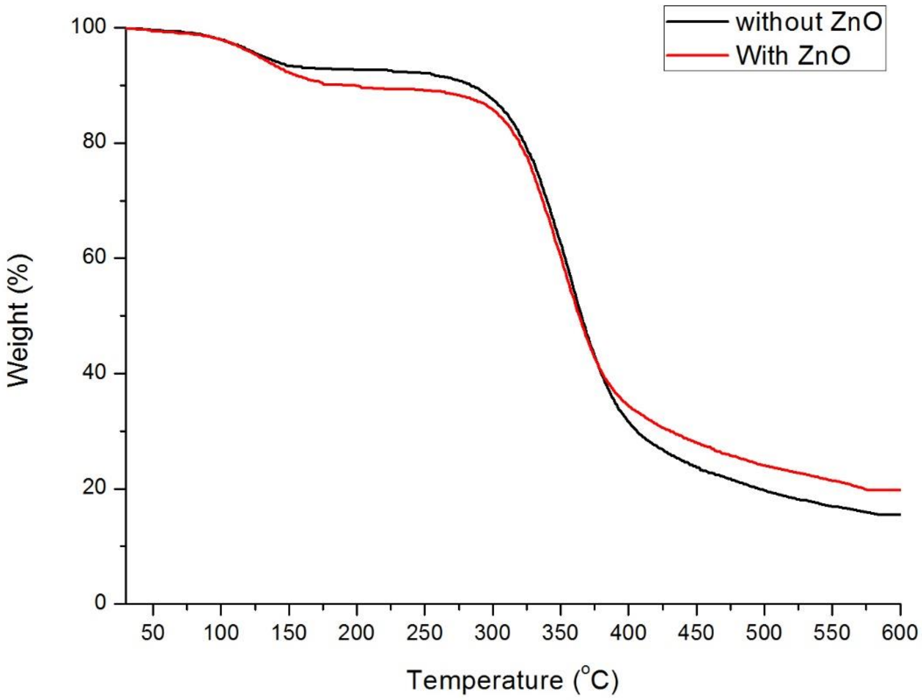

Figure 4-7 TGA thermograms of alkyd/epoxy blend and alkyd/epoxy/ZnO nanocomposite

The TGA was performed to investigate the thermal resistance of the resins by recording the percentage weight loss of the cured samples. This was performed to determine whether the influence of chain length affects the thermal resistance of the resin. The samples were heated at a uniform rate from 30 to 600 °C in inert condition. The thermogravimetric curves in Figure 4-7 show the significant improvement in thermal stability of the nanocomposite is observed by the incorporation of ZnO nanoparticles. The initial degradation temperature for the neat blend of alkyd/epoxy resin and alkyd/epoxy/ZnO nanocomposites starts at 300 °C. At temperature of 575 °C, the sample stops degrade. With the incorporation of ZnO nanoparticles, the initial degradation temperature increase. This can be attributed to the heat shielding effect of ZnO. The homogenous dispersion of nanoparticle within the polymer matrix provides a thermal barrier, releasing combustible volatiles during decomposition.

4.7 *Blending of alkyd/epoxy resin*

To obtain the optimal ratio of alkyd to epoxy blend, effect of alkyd/epoxy ratio was analysed by DSC. Table 4-2 shows the result of DSC measurements of different ratio alkyd/epoxy resin at constant heating rate of 10°C/min. It can be seen that, ΔH_{Total} value increased for the first three data and decreased afterwards. Sample A/E (40:60) exhibited highest ΔH_{Total} among others samples. It is also observed that the temperature of the curing exotherm (T_p) increased at A/E (0:100) to A/E (20:80), A/E (40:60) to A/E (50:50) and A/E (60:40) to A/E (80:20). The glass transition temperature (T_g) shows the trend of increasing from 73.11 °C to 87.66 °C for alkyd/epoxy ratio from 0:100 to 80:20.

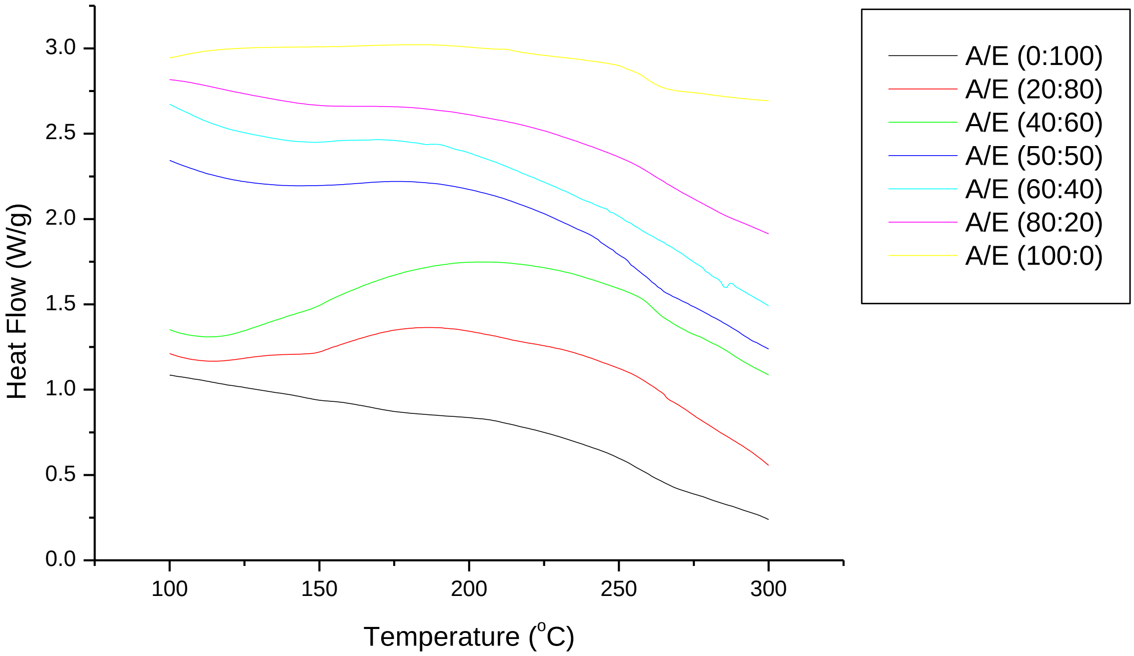

Figure 4-8 Dynamic DSC thermograms of alkyd/epoxy blend at different ratio of epoxy/alkyd obtained at scanning rate of 10°C/min

Table 4-2 Results of DSC measurements of different ratio of alkyd/epoxy

Resins	T_g (°C)	T_p (°C)	ΔH_{Total} (J/g)
A/E (0:100)	73.11	212.52	216.7
A/E (20:80)	84.66	253.32	320.2
A/E (40:60)	82.84	211.26	370.5
A/E (50:50)	86.96	212.82	195.5
A/E (60:40)	86.23	198.98	197.7
A/E (80:20)	87.66	224.87	136.7
A/E (100:0)	76.36	193.04	127.0

4.8 *Effect of ZnO nanoparticle on alkyd resin*

Table 4-3 shows the results of DSC measurements of alkyd at different weight percentage of ZnO nanoparticles. The effect of ZnO on alkyd resin can be clearly seen from the DSC curve shown on Figure 4-9 below. The curing peak can be observed with the incorporation of different weight % of ZnO.

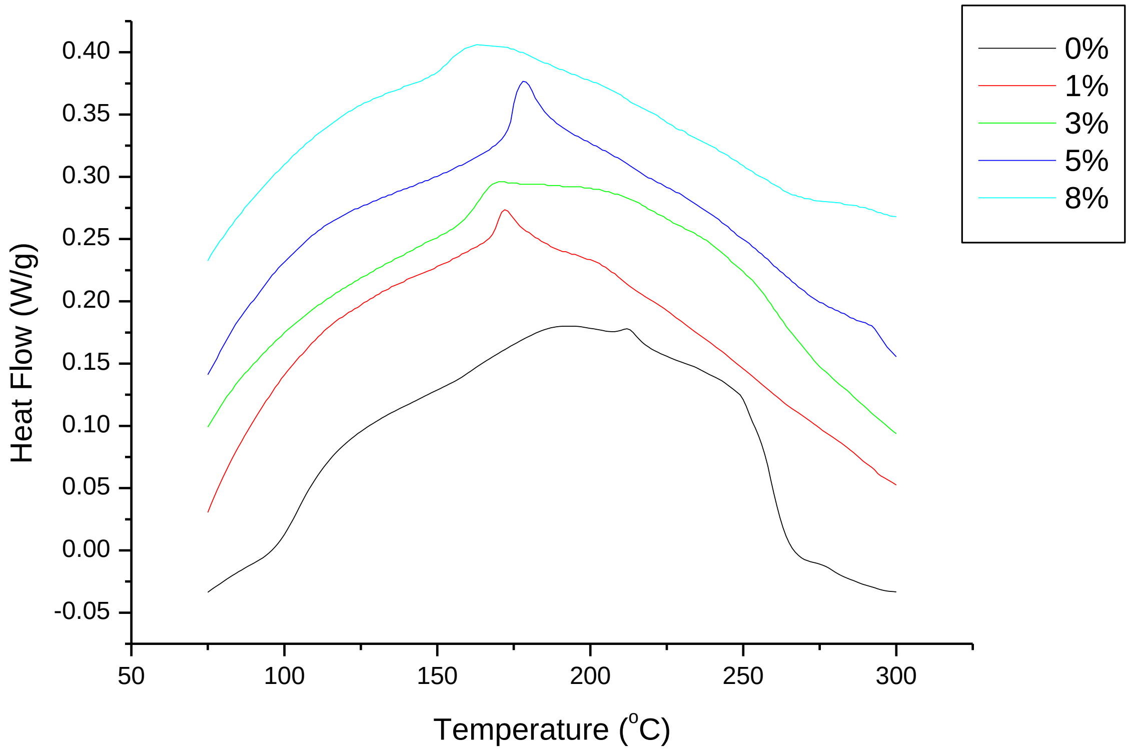

Figure 4-9 Dynamic DSC thermograms of alkyd/ZnO blend at different weight % of ZnO nanoparticle obtained at scanning rate of 10°C/min

Table 4-3 Results of DSC measurements of alkyd at different weight percentage of nano ZnO

Sample	ZnO (wt%)	T_p (°C)	ΔH_{Total} (J/g)
1	0	193.04	127.0
2	1	172.29	39.00
3	3	210.76	71.61
4	5	178.73	20.90
5	8	174.78	19.08

4.9 *Preparation of nanocomposite by incorporation of ZnO*

In order to obtain a desired value of the nanoparticle, stoichiometric ratio of alkyd and epoxy resin was mixed and then the effect of different weight percentage of ZnO nanoparticles was studied by DSC measurements. Table 4-4 presents the results of DSC measurements of alkyd/epoxy resin and the different weight percentage of ZnO. Effect of ZnO nanoparticles had significant influence on the curing mechanism and the final properties of the cured samples.

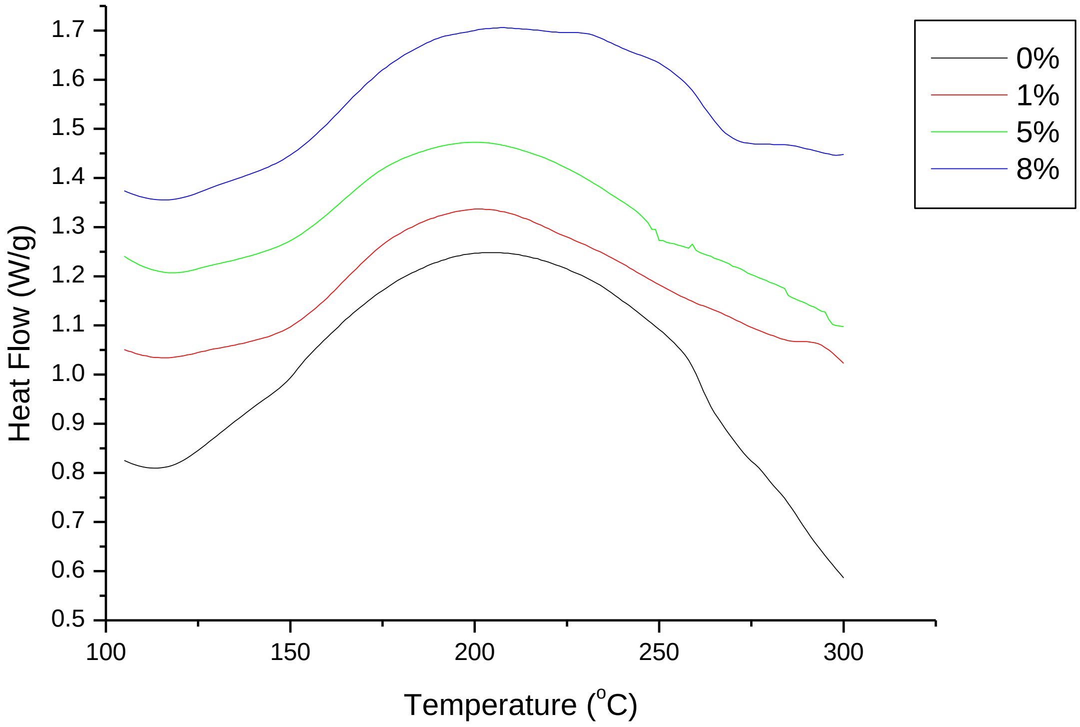

Figure 4-10 Dynamic DSC thermograms of alkyd/epoxy/ZnO nanocomposite blend at different weight % of ZnO nanoparticle obtained at scanning rate of 10°C/min

Table 4-4 Results of DSC measurements of alkyd/epoxy at different weight percentage of nano ZnO

Sample	ZnO (wt%)	T_g (°C)	T_p (°C)	ΔH_{Total} (J/g)
1	0	82.84	211.26	370.5
2	1	78.56	197.98	452.4
3	5	78.47	196.16	82.81
4	8	80.37	205.94	129.5

4.10 Non-isothermal DSC of alkyd/epoxy/ZnO blend at various heating rates

The heat flows of alkyd/epoxy blend cured with 1 wt % of ZnO from DSC are shown in Figure 4-11. From this figure, information about the nature of the curing reaction such as initial curing temperature and peak temperature of the resin at different heating rates can be derived. It can be observed that as the heating rate increases, the exothermic peak shift to higher temperatures. The results of DSC at different heating rates are listed in Table 4-5.

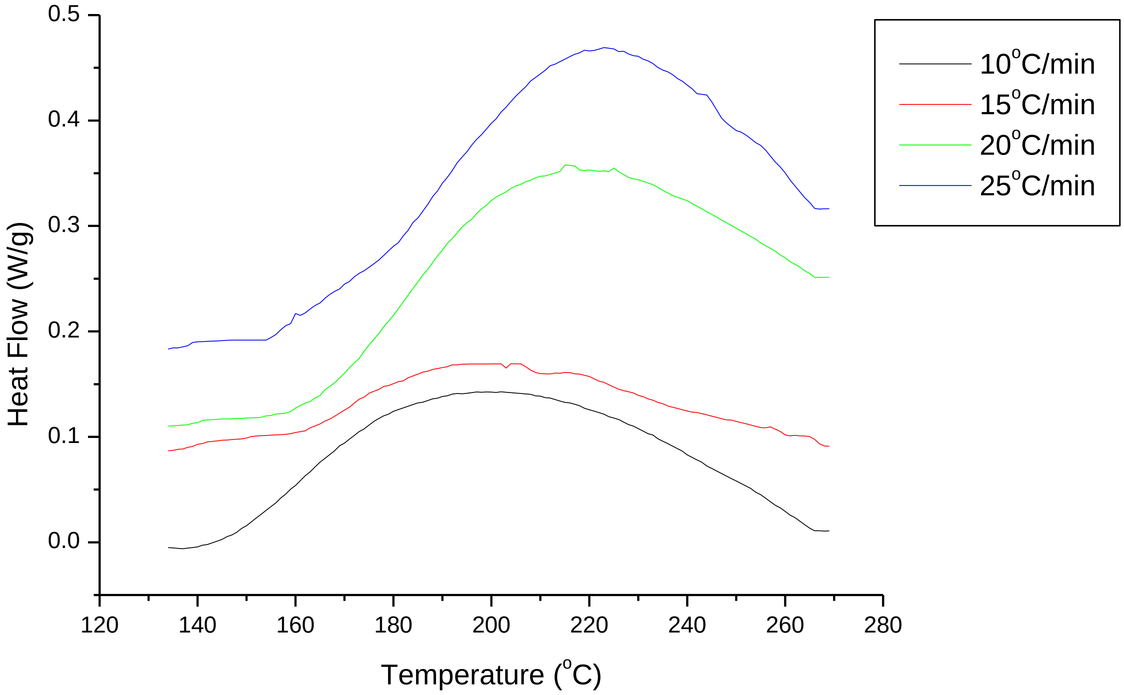

Figure 4-11 DSC curves of 40:60 alkyd/epoxy blend cured with 1wt % ZnO nanoparticle at different heating rate of 10, 15, 20 and 25 °C/min

Table 4-5 Data from the analysis of DSC measurements at different heating rate

Heating Rate (°C/min)	T_g (°C)	T_p (°C)	ΔH_{Total} (J/g)
10	78.56	197.98	452.4
15	87.61	204.59	360.7
20	93.18	215.22	325.1
25	101.15	223.32	340.0

4.11 Kinetic model

The data from DSC measurements were analysed with the Kissinger and Ozawa equation. The plot of –ln ($\frac{\beta}{T_p^2}$) against ($\frac{1}{T_p}$) is gives a straight line. Figure 4-12 displays the Kissinger plot.

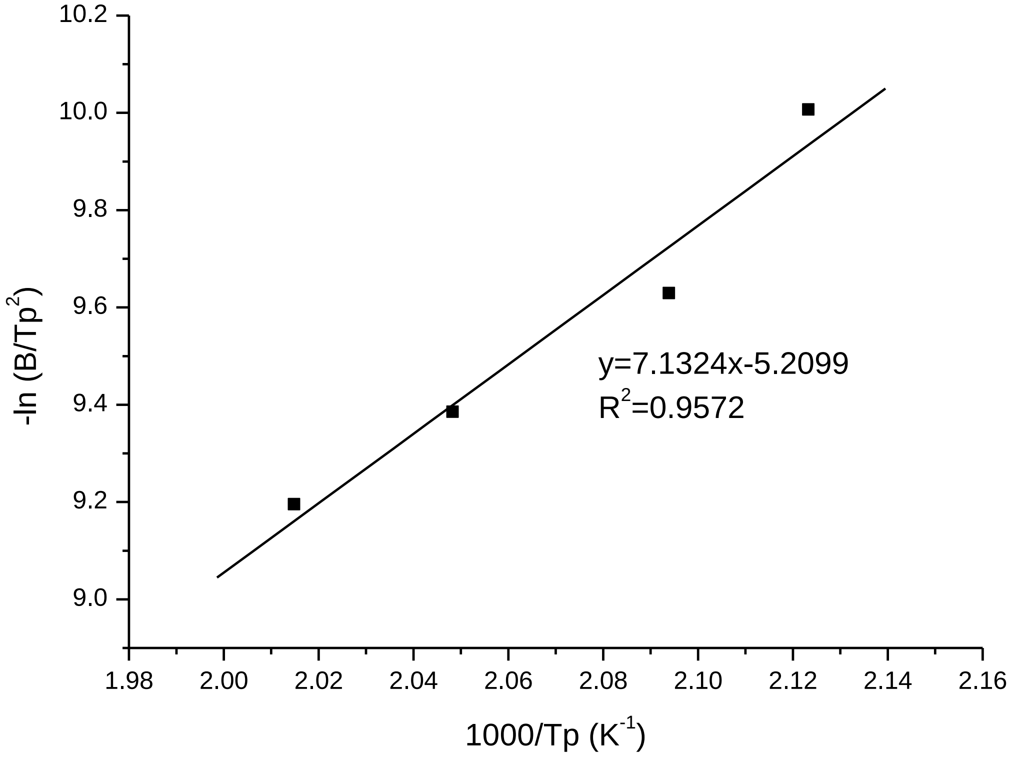

Figure 4-12 Kissinger method is applied to DSC exotherm for determination Ea

A linear regression analysis suggest that, to a good agreement, the calculated value of Ea is 59.30 kJ/mol.

The activation energy can be calculated using Ozawa method as shown in Figure 4-13.

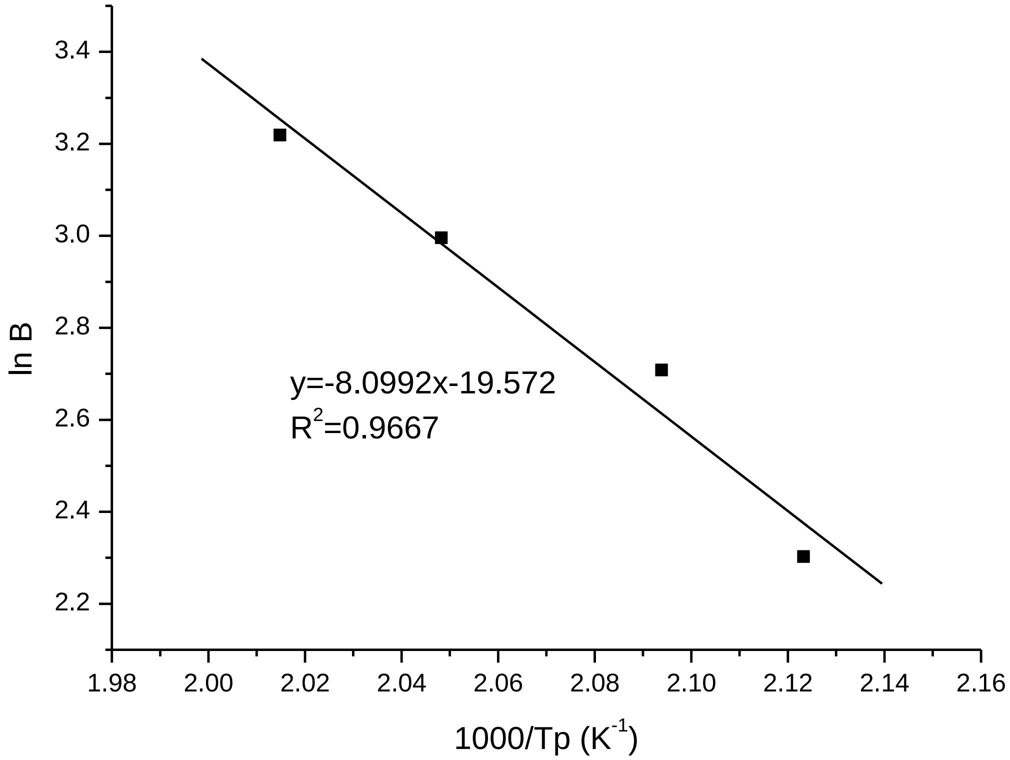

Figure 4-13 Ozawa method is applied to DSC exotherm for determination Ea

A plot of ln (β) against $\frac{1}{T_p}$ gives a linear plot with a slope of $\frac{1.052\,E_a}{R}$. The calculated activation energy based on Ozawa is 64.01 kJ/mol. From R^2 value, it shows that Ozawa method is more fit compared to Kissinger.

5 CONCLUSION

5.1 *Conclusion*

ZnO nanoparticle was prepared using a sol gel method. The XRD analysis indicate that highly pure ZnO formed was obtained. Thermal stability of the nanocomposites increased noticeably by the incorporation of ZnO nanoparticles. Alkyd/epoxy/ZnO blend was successfully prepared by mechanical blending. DSC non-isothermal was used in determining the curing kinetic of the blend. Ozawa and Kissinger kinetic models was used to calculate the E_a by using DSC data. The activation energy obtained by Ozawa is chose based on the R^2 value. All the results from the analysis deduce a conclusion that ZnO nanoparticles have significant effects on the performance characteristic of the alkyd/epoxy blends.

5.2 *Future work*

For the future work, further study is needed for the effects of ZnO on mechanical properties study such as tensile, flexural and impact strength. The DSC analysis on the nanocomposite is needs to further understand its thermal behaviour. Apart from that, Raman spectroscopy technique is needed to further investigate the influence of ZnO in the blend sample.

REFRENCES

Abdollah, O., Leonardo, C., & Abbas, A. (2009). Materials Chemistry and Physics. *The effects of alumina nanoparticle on the properties of an epoxy resin system*, 145-150.

Ahmad, M., Mohammad, R., & Mohammad, R. (2012). Modified Sherrer Equation to Estimate More Accurately Nano-Crystallite Size Using XRD . *World Journal of Nano Sized and Engineering*, 154-160.

Arabli, V., & Aghili, A. (2013). Effect of Silica Nanoparticles on the Curing Kinetics of Epoxy Vinyl Ester Resin. *Proceedings of the International Conference Nanomaterials: Applications and Properties*, 1-4.

Babita, B., Kishore, D., & Manorama, S. (2006). Sens. Actuators B. *Hydrothermal synthesis of highly crystalline ZnO nanoparticles: a competitive sensor for LPG and EtOH*, 676-682.

Badhuri, S., & Badhuri, S. (1997). Nanostrct. Mater. *Enhanced low temperature toughness of Al2O3-ZrO2 nano/nano composites*, 755-763.

Blaise, V., Ogunniyi, D., Ongoka, P., Moussounga, J., & Ouamba, J. (2012). Physico-chemical Properties of Alkyd Resins and Palm Oil Blends. *Malaysian Polymer Journal*, 42-45.

Bora, M., Deka, R., Ahmed, N., & Kakati, D. (2014). Karanja (Millettia pinnata (L.) Panigrahi) seed oil a s a renewable raw material for the synthesis of alkyd resin. *Industrial Crops and Products*, 106-114.

Bora, M., Gogoi, P., Deka, D., & Kakati, D. (2014). Synthesis and characterization of yellow oleander (Theveria peruviana) seed oil-based alkyd resin. *Ind. Crops Prod.*, 721-728.

Chang, S., Yoon, S., Park, H., & Sakai, A. (2002). Mater. Lett. *Luminescence properties of Zn nanowires prepared by electrochemical etching*, 432-436.

Deka. D.C., B. S. (2011). High quality biodiesel from yellow oleander (Thevetia peruviana) seed oil. *Biomass Bioenergy*, 1797-1803.

Deligny, P., Tuck, N., & Oldring, P. (2000). *Resins for Surface Coatings.* Chichester: John Wiley and Sons.

Dutta, N. K. (2004). Synthesis and characterizationof polyester resins based on Nahar seed oil. *Prog. Org. Coat. 49*, 146-152.

E., A., Z., Y., S.K., K., M., I., & J., S. (2009). Characteristic and Composition of Jatropha Curcas Oil Seed from Malaysia and its Potential as Biodiesel Feedstock. *European Journal of Scientific Research* , 396-403.

Edem, D. (2002). Palm oil: Biochemical, physiological, nutritional, hematological, and toxicological aspects: A review. *Kluwer Academic Publishers,* 319–341.

Gogoi, P., Boruah, M., Bora, C., & Dolui, S. (2014). Prog. Org. Coat. 87.

Gogoi, P., Saikia, B., & Dolui, S. (2014). Effect of nickel oxide (NiO) nanoparticles on the performance characteristics of the jatropha oil based alkyds and epoxy blends. *Applied Polymer Science*, 2-3.

Ikhuoria, E., Okieimen, F., Obazee, E., & Erhabor, T. (2011). Academic Journals. *Synthesis and characterization of styrenated rubber seed oil alkyd*, 1913-1918.

Issam, A., NurulKhizrien, A., & Mazlan, I. (2011). Physical and Mechanical Properties of Different Ratios of Palm Oil-Based Alkyd/Epoxy Resins. *Polymer. Plas. Technol. Eng*, 1256-1261.

Jubsilp, C., Damrongsakkul, S., & Takeichi, T. (2006). *Thermochim. Acta*, 131-140.

Khandelwal, S., & Chauhan, Y. (2012). J. Chem. Pharm. Res. *Biodiesel production from non-edible oils: a review*, 4219-4230.

Khorsand, Z., Abid, A., Majid, W., Wang, H., Yousefi, R., Golsheikh, M., & Ren, Z. (2013). Ultrasonic Sonochemistry. *Sonochemical synthesis of hierarchical ZnO nanostructures*, 395-400.

Kooti, M., & Nagdhi Sedish, A. (2013). J. Chem. *Microwave-assisted combustion synthesis of ZnO nanoparticles*.

Kumar, M., Yaakob, Z., Maimunah, S., Siddaramaiah, & Abdullah, S. (2010). Synthesis of alkyd resin from non-edible jatropha seed oil. *J. Polym. Environ. 18,* 539-544.

Kumar, S., & Purushothaman, K. (2012). High FFA rubbers seed oil as an alternative fuel or diesel engine-an overview. *Int. J. Eng. Sci. 1*, 16-24.

Lamas, D., Lascalea, G., & Walsoc, N. (1998). J. Eur. Ceram. Soc. *Synthesis and characterization of nanocrystalline powders for partially stabalized zirconia ceramics*, 1217-1221.

Ling, J. M. (2014). Novel poly (alkyd-urethane)s from vegetable oils: sysnthesis and properties. *Ind. Crops Prod. 52*, 74-84.

Montu, M., Riblu, D., Nuruddin, A., & Dilip, K. (2014). Industrial Crops and Products. *Karanja (Millettia pinnata (L.) Panigrahi) seed oil as a renewable raw material for the synthesis of alkyd resin*, 106-114.

Ni, Y., Wei, X., Hong, J., & Ye, Y. (2005). Master Sci. Eng., B, Solid State Mater. Adv. Technol. *Hydrothermal synthesis and opyical properties of ZnO nanorods*, 42-47.

Odetoye, T. O. (2012). Improving Jatropha curcas Linnaeus oil alkyd drying properties. *Progress in Organic Coatings*, 1.

Odetoye, T., Ogunniti, D., & Olatunji, G. (2010). Preparation and evaluation of Jatropha curcas Linneaus seed oil alkyd resins. *Industrial Crops and Products*, 225-230.

Ogunniyi, D., & Odetoye, T. (2008). Bioresour. Technol. *Preparation and evaluation of tobacco seed oil-modified alkyd resins*, 1300-1304.

Omid, Z., Mostafavi, S., Fatemeh, R., Aminreza, K., Amin, H., Karim, Z., & Mehrab, S. (2011). The effect of zinc oxide nanoparticles on thermo-physical properties of diglycidyl ether of bisphenol A/2,2'-Diamino-1,1;-binaphthalene nanocomposites. *Thermochimia Acta*.

Pasari, M. S., & Chandra, S. (1979). Pigm. Resin Technol. 12.

Pronob, G. B., & Swapan, K. (2014). Effect of Nickel Oxide (NiO) Nanoparticels on the Performance Characteristics of the Jatropha Oil Based Alkyd and Epoxy Blends. *Applied Polymer Science*, 1-9.

Radicevic, R. Z., & Simendic, J. K. (2005). J. Serb. Chem. Soc. 539.

Rajesh, D., Vara Lakshmi, B., & Sunandana, C. (2012). Physica B-Cond. Mater. *Two-step synthesis and characterization of ZnO nanoparticles*, 4537-4539.

Ristiac, M., Musiac, S., Ivanda, M., & Popoviac, S. (2005). J. Alloys Compd. *Sol-gel synthesis and characterization of nanocrystalline ZnO powders*, L1-L4.

Saravari, O., Phapant, P., & Pimpan, V. (2005). Synthesis of water-reducible acrylic-alkyd resins based on modified palm oil. *J. Appl. Polym. Sci*, 1170-1175.

Scarisoreanu, N., Metai, D., Dinescu, G., Epurescu, G., Ghica, C., Nistor, L., & Dinescu, M. (2005). Appl. Surf. Sci. *Properties of ZnO thin film prepared by radio-ferquency plasma beam assisted laser ablation*, 518-525.

Shetty, A., & Nanda, K. (2012). Appl. Phys. A. *Synthesis of zinc oxide porous structures by anodisation with water as an electrolyte* , 151-157.

Singh, O., Kohli, N., & Singh, R. (2013). Sens. Actuators B. *Precursor controlled morphology of zinc oxide and its sensing behavior*, 149-154.

Surabhi, S., Putcha, V., Vannka, R., & Gollapalli, N. (2013). International Nano Letters. *Synthesis, characterization and optical properties of zinc oxide nanoparticles*.

Trivedi, M., & Mann, A. (1991). Studies on blends of alkyd resin and petroleum resin. *Paintindia*, 57-62.

Urban, D., & Owada, T. (2012). Bio-toner Containing Bio-resin, Method for Making the Same, and Method for Printing With Bio-toner Containing Bioresin. *Patent Application Publication*, 12.

Vafaee, M., & Ghamsari, M. S. (2006). Materials Letters. *Preparation and characterization of ZnO nanoparticles by a novel sol-gel route*, 3265-3268.

Vasquez, A., Lopez, I., & Gomez, I. (2013). J. Mater. Sci. *Growth mechanism of one-dimensional zinc sulfide nanostructures through electrophoretic deposition*, 2701-2704.

Wang, R., & Tsai, C. (2009). Appl. Phys. A. *Efficient synthesis of ZnO nanoparticles, nanowalls, and nanowires by thermal decomposition of zinc acetate at low temperature*, 241-245.

Wang, T., Alarcon, C. D., Goikoetxea, M., Beristain, I., Paulis, M., Barandiaran, M. J., . . . Keddie, J. L. (2010). Langmuir. 14323.

Wu, J., & Liu, S. (2002). Adv. Mater. *Low-temperature growth of well-aligned ZnO nanorods by chemical vapor deposition*, 215-218.

Xia, Y., & Larock, R. (2011). Macromol. Rapid Commun. 1331.

APPENDICES

Figure A1: Mixing process to produce ZnO nanoparticle

Figure A2: Filtration and washing of ZnO solution

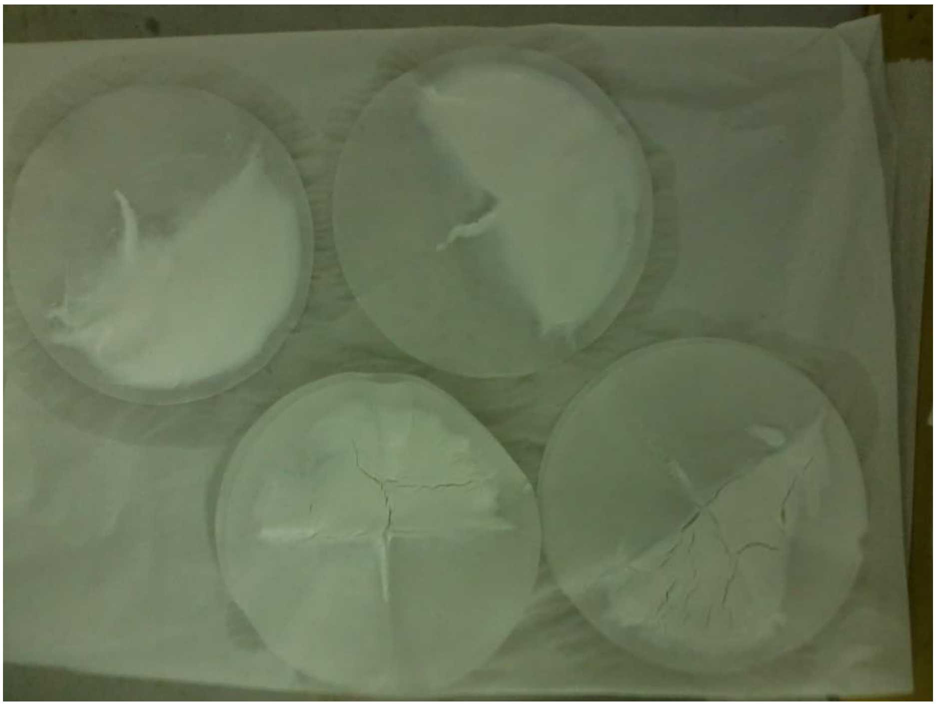

Figure A3: Filtered solid of ZnO

Figure A4: Two stages alcoholysis-polysterification process